
Advanced Sign Language Video Generation with Compressed and Quantized Multi-Condition Tokenization

Cong Wang^{1*} Zexuan Deng^{1*} Zhiwei Jiang^{1†} Yafeng Yin^{1†} Fei Shen²
 Zifeng Cheng¹ Shiping Ge¹ Shiwei Gan¹ Qing Gu¹

¹ State Key Laboratory for Novel Software Technology, Nanjing University

² National University of Singapore

{cw, dengzx}@smail.nju.edu.cn {jzw, yafeng}@nju.edu.cn
 shenfei29@nus.edu.sg {chengzf, shipingge, sw}@smail.nju.edu.cn
 guq@nju.edu.cn

Abstract

Sign Language Video Generation (SLVG) seeks to generate identity-preserving sign language videos from spoken language texts. Existing methods primarily rely on the single coarse condition (*e.g.*, skeleton sequences) as the intermediary to bridge the translation model and the video generation model, which limits both the naturalness and expressiveness of the generated videos. To overcome these limitations, we propose SignViP, a novel SLVG framework that incorporates multiple fine-grained conditions for improved generation fidelity. Rather than directly translating error-prone high-dimensional conditions, SignViP adopts a discrete tokenization paradigm to integrate and represent fine-grained conditions (*i.e.*, fine-grained poses and 3D hands). SignViP contains three core components. (1) Sign Video Diffusion Model is jointly trained with a multi-condition encoder to learn continuous embeddings that encapsulate fine-grained motion and appearance. (2) Finite Scalar Quantization (FSQ) Autoencoder is further trained to compress and quantize these embeddings into discrete tokens for compact representation of the conditions. (3) Multi-Condition Token Translator is trained to translate spoken language text to discrete multi-condition tokens. During inference, Multi-Condition Token Translator first translates the spoken language text into discrete multi-condition tokens. These tokens are then decoded to continuous embeddings by FSQ Autoencoder, which are subsequently injected into Sign Video Diffusion Model to guide video generation. Experimental results show that SignViP achieves state-of-the-art performance across metrics, including video quality, temporal coherence, and semantic fidelity. The code is available at <https://github.com/umnoob/signvip>.

1 Introduction

Sign language, as a visual language, serves as the primary communication medium for deaf individuals. Early research focused on Sign Language Recognition (SLR) [32, 45, 90], Translation (SLT) [5, 20, 42, 14], or Production (SLP) [58, 56, 60, 86, 83]. More recently, Sign Language Video Generation (SLVG) [57, 61, 47, 69] has gained increasing attention, which aims to generate realistic and expressive sign language videos from spoken language texts, preserving the unique identity of a target signer, as

*Equal contribution.

†Corresponding author.

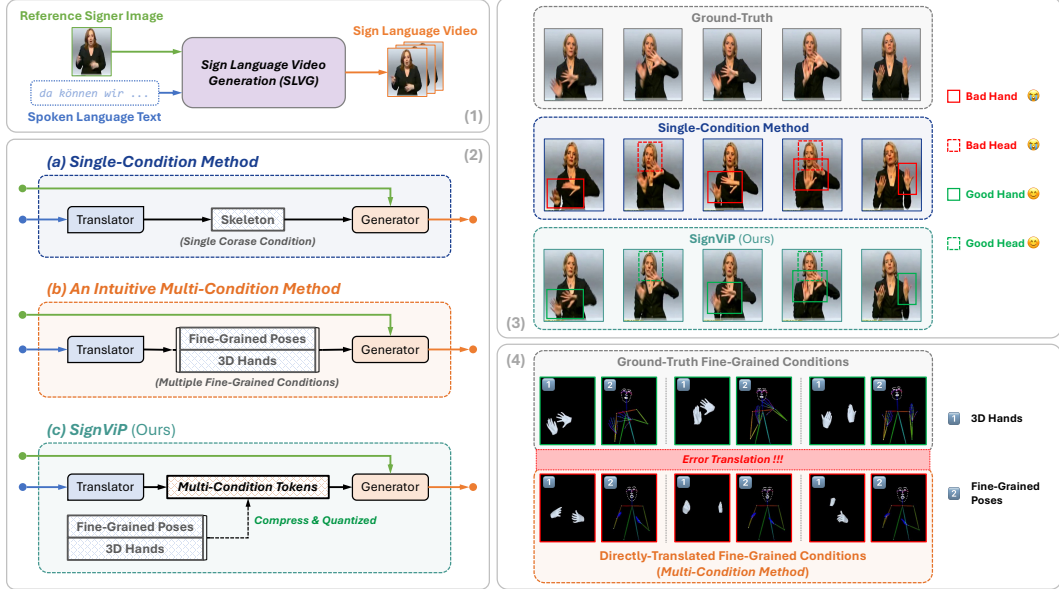


Figure 1: (1) The illustration of SLVG task. (2) The pipeline comparison between existing SLVG methods (*i.e.*, single-condition method and multi-condition method) and our SignViP. (3) Single-condition methods struggle to accurately capture the naturalness and expressiveness of sign language videos. (4) Multi-condition methods are prone to translation errors for fine-grained conditions.

shown in Figure 1(1). This growing interest is driven by its potential applications in accessibility technologies, educational tools, immersive communication systems, *etc.*

SLVG presents a challenging problem due to the lack of explicit spatial or temporal alignment between the input (*i.e.*, the spoken language texts) and output (*i.e.*, the sign language videos) modalities. To address this, current SLVG methods focus on leveraging synchronized auxiliary conditions as an intermediary to align these two modalities. As shown in Figure 1(2a), most of the existing SLVG methods [57, 61] leverage skeletal sequences as an intermediary to bridge a text-to-skeleton translation model (*i.e.*, an SLP model) and a skeleton-to-video generation model. Because the generative model is only guided by a single coarse condition (*e.g.*, skeleton), such single-conditional methods struggle with the naturalness and expressiveness of the generated videos, particularly in capturing facial expressions and figure movements, as illustrated in Figure 1(3).

Recent advancements in human video generation have shown that incorporating fine-grained conditions (*e.g.*, dense pose [84] or 3D models [9, 82]) or leveraging multiple conditions (*e.g.*, depth combined with optical flow [85]) can substantially improve generative fidelity. Inspired by these, we consider whether multiple fine-grained conditions can be introduced to enhance the quality and expressiveness of generated sign language videos. As shown in Figure 1(2b), one intuitive solution is to extend the single-conditional methods by considering multiple fine-grained conditions as intermediaries, where a multi-condition translation model can directly predict capable of achieving multiple fine-grained conditions. However, as shown in Figure 1(4), we observe that directly translating such attributes is challenging due to their high-dimensional nature and susceptibility to errors. This raises an important question: *How can we overcome the challenges in the translation of multiple fine-grained conditions to further advance SLVG?*

To address the challenges, we propose **SignViP**, a novel framework designed to advance SLVG by incorporating multiple fine-grained conditions for enhanced generation fidelity. As shown in Figure 1(2c), instead of directly translating high-dimensional conditions from spoken language texts, SignViP adopts a discrete tokenization paradigm to effectively integrate and represent these fine-grained conditions. Central to this framework is the construction of a **discrete multi-condition token space**, which bridges fine-grained conditions (*e.g.*, fine-grained poses and 3D hands) with the dynamics of sign language video frames. The framework consists of three key components: (1) **Sign Video Diffusion Model** is jointly trained with a multi-condition encoder using denoising loss to

generate continuous embeddings that encapsulate fine-grained motion and appearance details; (2) **Finite Scalar Quantization (FSQ) Autoencoder** is trained with reconstruction loss to compress and quantize the continuous embeddings into discrete tokens, enabling highly dense representation for the conditions; (3) **Multi-Condition Token Translator** is built upon an autoregressive model to translate spoken language text to discrete multi-condition tokens. During inference, the spoken language text is first translated into discrete multi-condition tokens by Multi-Condition Token Translator. These tokens are then decoded back into continuous embeddings by FSQ Autoencoder, which are subsequently injected into Sign Video Diffusion Model to guide sign language video generation. Our experimental results demonstrate that SignViP achieves state-of-the-art performance across multiple evaluation metrics, including video quality, temporal coherence, and semantic fidelity.

Our main contributions are summarized as follows:

- We introduce SignViP, a novel framework for Sign Language Video Generation (SLVG) that incorporates multiple fine-grained conditions for improved video quality and expressiveness.
- We propose a discrete tokenization paradigm through the construction of a discrete multi-condition token space to bridge fine-grained conditions with the dynamics of sign language video frames.
- The experiments validate the effectiveness of SignViP, demonstrating state-of-the-art performance across diverse metrics.

2 Related Works

Sign Language Video Generation. Sign Language Video Generation (SLVG) aims to generate identity-preserving sign language videos from spoken language texts. Early methods decompose the task into two consecutive sub-tasks [57, 61], which are the text-to-skeleton translation (*i.e.*, SLP) and the skeleton-to-video generation. SignGAN [57] first employs a transformer [76] with a mixture density formulation to translate spoken language text to skeletal sequence. Then, a GAN-based [17] skeleton-conditioned human synthesis model is introduced to generate sign language videos. FS-Net [61] extends SignGAN by predicting the temporal alignment to a continuous signing sequence. Because the single condition focuses solely on capturing basic pose structures while neglecting fine-grained details, the generated videos tend to appear less natural and expressive. SignGen [47] seeks to address this limitation through a novel end-to-end pipeline that integrates multi-condition guidance, including optical flow, pose, and depth. However, SignGen suffers from training-inference inconsistency, which leads to suboptimal results. In this paper, we aim to develop a framework that leverages multiple fine-grained conditions to enhance the quality and expressiveness of generated sign language videos.

Human Video Generation. Human video generation has advanced significantly with the deep generative models. Early approaches, such as Pix2PixHD [80] and vid2vid [79], leveraged GANs [17] to generate realistic images and videos from the structured inputs. Several works have also explored the human pose generation, conditioning on the whole body [2, 38, 40, 63], face [10, 33], or hands [73, 35]. However, GAN-based methods often suffer from mode collapse and optimization challenges. More recently, diffusion models [70, 28, 67, 78, 64, 68] have emerged as a robust alternative, producing high-quality images or videos with greater stability. Most prior diffusion-based approaches rely on ControlNet [88] and OpenPose [7] to process each video frame independently, neglecting the temporal consistency and leading to the inevitable flickering artifacts. Pose-guided diffusion models [62, 29, 77, 91, 65, 66] addresses this issue by generating temporally consistent human videos while preserving appearance fidelity. Furthermore, recent research shows that incorporating fine-grained conditions, such as dense pose [84] or 3D models [9, 82], or leveraging multiple complementary conditions, such as depth and optical flow [85], can significantly enhance generative fidelity. Building on these advancements, we aim to harness state-of-the-art diffusion-based methods alongside multiple fine-grained conditions to advance SLVG further.

3 Methodology

3.1 Preliminary

Diffusion Models. As a class of the generative models, the diffusion models [70, 28] consists of two processes, which are the diffusion process and the denoising process, respectively. In the diffusion

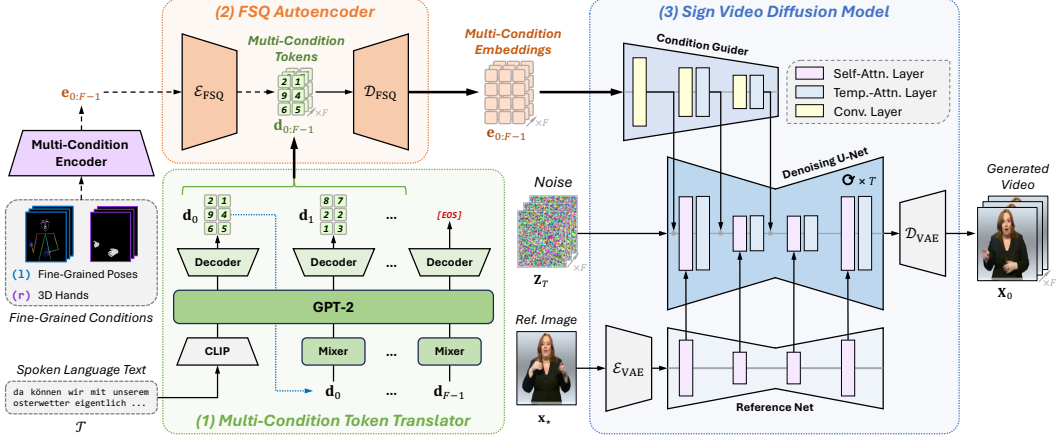


Figure 2: Framework of our SignViP for sign language video generation (SLVG). (1) The spoken language text is translated into the multi-condition tokens by Multi-Condition Token Translator. (2) These tokens are decoded by FSQ Autoencoder into multi-condition embeddings, which are equivalent to the embeddings of multiple fine-grained conditions (*i.e.*, fine-grained poses and 3D hands) generated by a multi-condition encoder. (3) The embeddings are injected into Sign Video Diffusion Model to guide the generation of sign language videos.

process, the Gaussian noise is iteratively added to degrade the input sample over T steps until the sample becomes completely random noise. In the denoising process, a denoising model is used to iteratively generate a sample from the sampled Gaussian noise. When training, given an input sample \mathbf{x}_0 and condition \mathbf{c} , the denoising loss is defined as

$$\mathcal{L}_{\text{denoise}} = \mathbb{E}_{\mathbf{x}_0, \epsilon \sim \mathcal{N}(\mathbf{0}, \mathbf{I}), \mathbf{c}, t} \|\epsilon_\theta(\mathbf{x}_t, \mathbf{c}, t) - \epsilon\|^2. \quad (1)$$

Among them, $\mathbf{x}_t = \sqrt{\alpha_t} \mathbf{x}_0 + \sqrt{1 - \alpha_t} \epsilon$ is the noisy sample at timestep $t \in [1, T]$, where α_t is a predefined scalar from the noise scheduler. ϵ is the added noise. ϵ_θ is the denoiser with the learnable parameters θ , which predicts the noise to be removed from the noisy sample. Latent Diffusion Models (LDMs) [55] stands out as one of the most popular diffusion models. It performs the two processes in the latent space, which is encoded by a Variational Auto-Encoder (VAE) [31, 54].

Finite Scalar Quantization. Finite Scalar Quantization (FSQ) [41] is a concise quantization technique to compress continuous values into discrete values. FSQ can be an alternative of Vector Quantization (VQ) [18] in VQ-VAE [75]. Compared with VQ, FSQ does not suffer from codebook collapse and does not need complex machinery to learn expressive discrete representations. Specifically, given a scalar $z \in \mathbb{R}$ from the encoded latent, the quantized discrete value by FSQ is

$$f(z; L) = (L - 1)\sigma(z); \text{ FSQ}(z) \triangleq \text{rnd}(f(z; L)) \in [0, 1, \dots, L - 1]. \quad (2)$$

Among them, $\text{rnd}(\cdot)$ is round function. $\sigma(\cdot)$ is sigmoid function. L is the predefined quantization level. Through this process, each value z is enumerated, leading to a bijection from z to an integer in $\{0, 1, \dots, L - 1\}$. For a d -dimensional latent vector, the total codebook size is the product of L_i across all dimensions, resulting in $\prod_{i=1}^d L_i$ possible discrete representations.

3.2 Overview

Given a reference signer image \mathbf{x}_* and a spoken language text \mathcal{T} , SLVG aims to generate a sign language video \mathbf{X} with F frames, where the signer performs sign language accurately aligned with the semantics of the spoken language text. Specifically, the SLVG task can be formulated as $p_\theta(\mathbf{X}|\mathbf{x}_*, \mathcal{T})$, where θ is parameters of the SLVG model.

Due to the lack of explicit spatial or temporal alignment between \mathcal{T} and \mathbf{X} , current SLVG methods focus on leveraging synchronized auxiliary conditions (*e.g.*, skeletal sequence) as an intermediary to align them. Such pipeline paradigm can be formulated as

$$p_\theta(\mathbf{X}|\mathbf{x}_*, \mathcal{T}) = p_{\theta_{\text{gen}}}(\mathbf{X}|\mathbf{x}_*, \mathbf{C}) \cdot p_{\theta_{\text{tran}}}(\mathbf{C}|\mathcal{T}). \quad (3)$$

Among them, \mathbf{C} is the synchronized auxiliary conditions which spatially and temporally aligned with the target video frames. θ_{tran} is parameters of the text-to-condition translation model, while θ_{gen} is parameters of condition-to-video generation model.

To address the generation quality issues caused by relying on a single coarse condition, we introduce multiple fine-grained conditions as intermediaries. Specifically, we utilize fine-grained poses and 3D hands. Fine-grained poses capture the signer’s body posture and facial expressions, while 3D hands provide detailed and accurate descriptions of hand movements, even in the presence of occlusions. To avoid directly translating error-prone high-dimensional conditions, SignViP employs a discrete tokenization paradigm with effective integration and representation of these fine-grained conditions.

As shown in Figure 2, the spoken language text \mathcal{T} is first translated into the discrete multi-condition tokens $\mathbf{d}_{0:F-1}$ by the **Multi-Condition Token Translator**. The multi-condition tokens $\mathbf{d}_{0:F-1}$ are then decoded by the **FSQ Autoencoder** to continuous multi-condition embeddings $\mathbf{e}_{0:F-1}$, which are equivalent to the embeddings obtained from a multi-condition encoder that encodes multiple fine-grained conditions (*i.e.*, fine-grained poses and 3D hands). Finally, $\mathbf{e}_{0:F-1}$ are injected into **Sign Video Diffusion Model** to guide the sign language video generation (*i.e.*, animating the signer in reference image \mathbf{x}_\star). The overall pipeline of SignViP can be formulated as

$$p_\theta(\mathbf{X}|\mathbf{x}_\star, \mathcal{T}) = p_{\theta_{\text{gen}}}(\mathbf{X}|\mathbf{x}_\star, \mathbf{e}_{0:F-1}) \cdot p_{\theta_{\text{AE}}}(\mathbf{e}_{0:F-1}|\mathbf{d}_{0:F-1}) \cdot p_{\theta_{\text{tran}}}(\mathbf{d}_{0:F-1}|\mathcal{T}), \quad (4)$$

where θ_{gen} , θ_{AE} , and θ_{tran} denote parameters of Sign Video Diffusion Model, FSQ Autoencoder, and Multi-Condition Token Translator, respectively.

3.3 Construction of Multi-Condition Token Space

SignViP is trained with three steps to construct the multi-condition token space for the discrete tokenization paradigm.

Step I. We train Sign Video Diffusion Model with a multi-condition encoder (*i.e.*, a multi-layer convolution network) using a denoising loss to establish a connection between the conditions and the sign language videos. Specifically, multiple fine-grained conditions (*e.g.*, fine-grained poses and 3D hands) are encoded by the multi-condition encoder into the continuous multi-condition embeddings $\mathbf{e}_{0:F-1}$. These embeddings, along with the reference image \mathbf{x}_\star , serve as the guidance signals for Sign Video Diffusion Model to perform diffusion process. More details can be found in Section 3.4.

Step II. We train FSQ Autoencoder using a reconstruction loss to learn the compression and quantization of multi-condition embeddings $\mathbf{e}_{0:F-1}$. The encoder \mathcal{E}_{FSQ} of FSQ Autoencoder compresses and quantizes the embeddings $\mathbf{e}_{0:F-1}$ into discrete multi-condition tokens $\mathbf{d}_{0:F-1}$, while the its decoder \mathcal{D}_{FSQ} reconstructs $\mathbf{e}_{0:F-1}$ from $\mathbf{d}_{0:F-1}$. More details can be found in Section 3.5.

Step III. We train the Multi-Condition Token Translator to autoregressively translate spoken language text \mathcal{T} to the multi-condition tokens $\mathbf{d}_{0:F-1}$. More details can be found in Section 3.6.

3.4 Sign Video Diffusion Model

Sign Video Diffusion Model aims to generate sign language videos in a diffusion-based manner [70, 28] under the guidance of the reference image \mathbf{x}_\star and the continuous multi-condition embeddings $\mathbf{e}_{0:F-1}$. Inspired by the previous works [29, 91], as shown in Figure 2(3), Sign Video Diffusion Model consists of three modules: Condition Guider, Denoising U-Net, and Reference Net. Condition Guider and Reference Net respectively encode the multi-condition embeddings $\mathbf{e}_{0:F-1}$ and the reference image \mathbf{x}_\star to guide the Denoising U-Net.

Denoising U-Net is the backbone of the Sign Video Diffusion Model, which mirrors the architecture of Stable Diffusion (SD) v1.5 [55]. Each U-Net block includes a ResNet layer [22], a self-attention layer, and a temporal-attention layer [21]. The self-attention layer and the temporal-attention layer perform attention operation [76] along the spatial axes and the temporal axis, respectively.

Condition Guider is a lightweight guidance network that encodes $\mathbf{e}_{0:F-1}$, whose each block consists of convolution layers and a temporal attention layer. The output feature of each block is added to the corresponding block’s feature in the downsampling part of the Denoising U-Net.

Reference Net [29] shares the same architecture of SDv1.5 and operates in parallel with the Denoising U-Net. The reference image \mathbf{x}_\star is first encoded into the latent space by the VAE encoder \mathcal{E}_{VAE} ,

$\mathbf{z}_* = \mathcal{E}_{\text{VAE}}(\mathbf{x}_*)$. The encoded reference latent \mathbf{z}_* is then fed into the Reference Net. The output feature of the self-attention layer in each block of the Reference Net is spatially concatenated with the input feature of the self-attention layer in the corresponding block of the Denoising U-Net.

During training, the loss function is the extended denoising loss of Equation 1,

$$\mathcal{L}_{\text{denoise}} = \mathbb{E}_{\mathbf{Z}_0, \epsilon \sim \mathcal{N}(\mathbf{0}, \mathbf{I}), t} \|\epsilon_\theta(\mathbf{Z}_t; \mathbf{r}_*, \mathbf{E}, t) - \epsilon_t\|^2. \quad (5)$$

Among them, $\mathbf{Z}_0 = \mathcal{E}_{\text{VAE}}(\mathbf{X}_0)$ is the target latent which is encoded from the target video \mathbf{X}_0 . ϵ_θ is the Denoising U-Net. $\mathbf{r}_* = \mathcal{R}(\mathbf{z}_*)$ is the reference features, which are encoded by the Reference Net \mathcal{R} . $\mathbf{E} = \mathcal{C}(\mathbf{e}_{0:F-1})$ is the conditional features, which are encoded by the Condition Guider \mathcal{C} .

Considering that subtle pose variations in sign language videos carry important semantic meaning, the model needs to be robust to potential anomalies in the generated condition sequences. To address this, we propose *condition augmentation*. Specifically, each condition frame has a probability p of being randomly replaced with frames from other videos, deliberately introducing controlled disruptions in the temporal continuity. By exposing the model to these artificial discontinuities during training, we effectively enhance its robustness to unexpected conditional transitions.

The inference starts from the sampled Gaussian noise. Then, the diffusion scheduler (*e.g.*, DDIM [71]) is applied to generate images with multiple denoising steps. For each inference step, the noise prediction relies on Classifier-Free Guidance (CFG) [27]. Finally, the generated video is achieved from the latent by a VAE decoder \mathcal{D}_{VAE} .

3.5 FSQ Autoencoder

The FSQ Autoencoder is designed to establish a connection between the multi-condition embeddings $\mathbf{e}_{0:F-1}$ and the corresponding discrete tokens $\mathbf{d}_{0:F-1}$. The pre-trained multi-condition encoder first encodes multiple conditions to the continuous embeddings $\mathbf{e}_{0:F-1}$. These embeddings are subsequently compressed and quantized into $\mathbf{d}_{0:F-1}$ by the FSQ Autoencoder encoder \mathcal{E}_{FSQ} , which provides a compact representation for the Multi-Condition Token Translator. Finally, the FSQ Autoencoder decoder \mathcal{D}_{FSQ} dequantizes $\mathbf{d}_{0:F-1}$ and reconstructs $\mathbf{e}_{0:F-1}$. The training objective of the FSQ Autoencoder is an L2 reconstruction loss.

$$\mathcal{L}_{\text{FSQ-AE}} = \mathbb{E}_{\mathbf{e}_{0:F-1}} \|\mathcal{D}_{\text{FSQ}}(\mathcal{E}_{\text{FSQ}}(\mathbf{e}_{0:F-1})) - \mathbf{e}_{0:F-1}\|^2. \quad (6)$$

The architecture of the FSQ Autoencoder follows that of the VAE. Instead of applying variational Bayesian inference in the latent space, it performs the FSQ operation, as illustrated in Equation 2.

3.6 Multi-Condition Token Translator

Multi-Condition Token Translator is designed to translate the spoken language text \mathcal{T} into the discrete multi-condition tokens $\mathbf{d}_{0:F-1}$. Since sign language videos often exceed 100 frames, and each frame should maintain coherent temporal relationships without a strict internal order, we design a frame-level autoregressive model.

As shown in Figure 2(1), following previous works [86, 3], the spoken language text \mathcal{T} is firstly encoded by CLIP text encoder [49] to obtain semantic embeddings, which serve as the initial input hidden states of the GPT-2 model [48]. Each output hidden state of the GPT model is decoded through multiple parallel prediction heads to generate all tokens of the corresponding frame simultaneously. On the input side, tokens belonging to the same frame are mixed to obtain unified input hidden states. Unlike methods that require dedicated modules for video length prediction [83] or rely on real video lengths [58], Multi-Condition Token Translator naturally determines the video generation endpoint by producing an “[EOS]” token.

During training, given the pre-trained multi-condition encoder and FSQ Autoencoder encoder, the produced tokens are considered the ground-truth. The cross-entropy loss is computed between the predicted tokens $\hat{\mathbf{b}}_{0:F}$ and the ground-truth tokens $\mathbf{b}_{0:F}$ ³,

$$\mathcal{L}_{\text{AR}} = \frac{1}{F+1} \sum_{i=0}^F \text{CrossEntropy}(\hat{\mathbf{b}}_i; \mathbf{b}_i). \quad (7)$$

³Note that we use F instead of $F - 1$ here due to the inclusion of the additional endpoint token “[EOS]”.

To mitigate the exposure bias issue between training and inference, we employ a *scheduled sampling strategy*, wherein 40% of the input tokens are randomly replaced with arbitrary indices from the vocabulary during training. This approach improves the model’s robustness and generalization performance during inference.

4 Experiments

4.1 Experimental Settings

Datasets. We employ two sign language datasets for experiments. (1) *RWTH-2014T* [5] is a German sign language dataset. It comprises 8,257 sign language videos. The dataset is divided into 7,096 training samples, 519 validation samples, and 642 test samples. To align with the $8\times$ downsampling rate of VAE, the frame size was resized from 260×210 to 272×224 . (2) *How2Sign* [11] is an American sign language dataset. It includes 2,456 sign language videos. Using the provided timestamps, we segmented the videos to create a sentence-level dataset. This dataset consists of 31,128 training samples, 2,322 test samples, and 1,741 validation samples. The frame size is set to 512×512 .

Evaluation Metrics. To evaluate semantic consistency, we utilize the back-translation metrics following ProTran [58]. Specifically, we train an SLT model [6] to translate sign language videos or poses back into texts. The back-translated text is then compared with the ground-truth text with metrics of *BLEU* [44] and *ROUGE-L* [34]. To provide a more comprehensive evaluation of back-translated texts, we further employ the *COMET* [52, 51] metric, which is specifically designed to predict human judgments of machine translation quality. COMET is widely used for machine translation tasks [19, 1, 24] and is considered more suitable than BLEU and ROUGE. To evaluate the video quality, we employ *FID* [26], *CLIP-FID*, *FVD* [74], and *Identity Similarity (IDS)*. Among them, CLIP-FID is a variation of FID that utilizes CLIP [49] embedding as the frame’s embedding. IDS measures the identity consistency between generated and ground-truth videos. It calculates the cosine similarity of face embeddings extracted using YOLO5Face [46] and Arc2Face [43]. To further investigate the generative capability of video diffusion models in addition to *FVD* [74], we employ frame-level metrics including *PSNR* [13], *SSIM* [81], and *LPIPS* [89], leveraging their suitability in scenarios where ground-truth videos are temporally aligned with the generated videos. Additionally, we introduce *Hand SSIM*, which measures SSIM specifically in the hand region for a more precise evaluation of the hand quality.

Implementation Details. In *Multi-Condition Token Translator*, we utilize a multilingual version of the CLIP model⁴ to enable handling of multiple spoken language texts effectively. In *FSQ Autoencoder*, the encoder and decoder follow the architecture of their counterparts in VAE. Specifically, FSQ Autoencoder applies 4 latent channels, with each channel having a quantization level of 5. Together, this results in a total vocabulary size of 625, computed as $5^4 = 625$ due to the combination of levels across all channels. In *Sign Video Diffusion Model*, both the Denoising U-Net and the Reference Net are initialized with Stable Diffusion v1.5⁵. The temporal-attention layers in the Denoising U-Net are initialized from AnimateDiff [21]. The condition augmentation rate is set to 0.001. During inference, Sign Video Diffusion Model utilizes a guidance scale of 3.5 for CFG. Additionally, the number of inference steps is configured to 50.

Training Details. The training of the three stages are conducted on 4 NVIDIA RTX A6000 GPUs using Adam optimizer [30], with each stage consisting of 50,000 training steps. The batch sizes of stage I, II, and III are 2, 16, and 16. Their learning rates are 1e-5, 5e-5, and 1e-6.

4.2 Comparison

Back-Translation Comparison. To quantitatively evaluate the semantic accuracy of the generated sign language videos, we perform two types of back-translation comparisons. Specifically, we respectively train a video-to-text translation model and a pose-to-text translation model to compare with SLVG methods and SLP methods [6]. For pose back-translation comparison, we extract pose sequences from the generated videos using OpenPose [7] and a 2D-to-3D mapping method [87]. As

⁴<https://huggingface.co/sentence-transformers/clip-ViT-B-32-multilingual-v1>

⁵<https://huggingface.co/stable-diffusion-v1-5/stable-diffusion-v1-5>

Table 1: Comparison of **video back-translation** performance.

| | RWTH-2014T | | | | | | How2Sign | | | | | |
|--------------------------------|--------------|--------------|--------------|-------------|--------------|---------------|--------------|-------------|-------------|-------------|--------------|---------------|
| | BLEU-1 | BLEU-2 | BLEU-3 | BLEU-4 | ROUGE | COMET | BLEU-1 | BLEU-2 | BLEU-3 | BLEU-4 | ROUGE | COMET |
| Ground-Truth | 33.06 | 20.81 | 15.00 | 11.90 | 34.27 | 0.6157 | 20.37 | 13.11 | 9.78 | 7.53 | 21.43 | 0.5882 |
| MoMP [59] + ControlNet [88] | 19.12 | 8.95 | 5.33 | 3.61 | 21.54 | 0.5033 | 12.53 | 5.59 | 3.48 | 2.31 | 13.72 | 0.5122 |
| MoMP [59] + AnimateAnyone [29] | 20.05 | 8.79 | 5.24 | 3.72 | 21.68 | 0.5091 | 13.65 | 5.82 | 3.39 | 2.25 | 14.15 | 0.5208 |
| SignGAN [61] | 17.41 | 7.93 | 4.67 | 3.16 | 19.64 | 0.4977 | 10.66 | 4.62 | 2.92 | 1.97 | 11.76 | 0.5104 |
| w/ AnimateAnyone [29] | 18.29 | 7.75 | 4.59 | 3.23 | 19.70 | 0.4928 | 11.82 | 4.85 | 2.83 | 1.92 | 12.12 | 0.5135 |
| SignGen [47] | 13.28 | 3.05 | 1.13 | 0.51 | 16.13 | 0.4086 | 8.21 | 1.91 | 0.64 | 0.41 | 9.54 | 0.4127 |
| SignViP (Ours) | 26.72 | 15.65 | 11.14 | 8.65 | 28.85 | 0.5608 | 16.21 | 9.36 | 6.28 | 5.04 | 16.99 | 0.5524 |

Table 2: Comparison of **pose back-translation** performance.

| | RWTH-2014T | | | | | | How2Sign | | | | | |
|-----------------------|--------------|--------------|-------------|-------------|--------------|---------------|--------------|-------------|-------------|-------------|--------------|---------------|
| | BLEU-1 | BLEU-2 | BLEU-3 | BLEU-4 | ROUGE | COMET | BLEU-1 | BLEU-2 | BLEU-3 | BLEU-4 | ROUGE | COMET |
| Ground-Truth | 30.99 | 18.36 | 12.83 | 9.87 | 31.02 | 0.5978 | 24.56 | 14.96 | 10.31 | 7.91 | 24.88 | 0.6250 |
| ProTran [58] | 17.96 | 8.99 | 5.64 | 4.07 | 20.97 | 0.5091 | 14.57 | 7.47 | 4.59 | 3.42 | 17.32 | 0.5549 |
| Adversarial [56] | 17.70 | 8.96 | 5.72 | 4.18 | 21.15 | 0.5127 | 14.76 | 7.15 | 4.66 | 3.48 | 17.84 | 0.5618 |
| MDN [60] | 18.06 | 9.30 | 6.06 | 4.52 | 21.44 | 0.5251 | 14.94 | 7.54 | 5.10 | 3.67 | 18.21 | 0.5685 |
| MoMP [59] | 20.55 | 10.98 | 7.02 | 5.14 | 23.75 | 0.5466 | 16.57 | 8.47 | 5.38 | 4.16 | 19.38 | 0.5802 |
| SignGAN [61] | 12.14 | 6.10 | 3.88 | 2.85 | 14.79 | 0.5123 | 10.86 | 5.27 | 3.30 | 2.62 | 13.19 | 0.5673 |
| w/ AnimateAnyone [29] | 12.36 | 6.23 | 4.01 | 2.97 | 14.93 | 0.5231 | 10.97 | 5.36 | 3.39 | 2.67 | 13.36 | 0.5315 |
| SignGen [47] | 10.42 | 2.42 | 0.89 | 0.38 | 12.68 | 0.4324 | 8.67 | 1.79 | 2.41 | 1.36 | 8.69 | 0.4413 |
| SignViP (Ours) | 21.94 | 10.06 | 6.32 | 4.61 | 22.67 | 0.5347 | 17.35 | 8.28 | 5.41 | 4.42 | 18.23 | 0.5738 |

shown in Table 1, in *video back-translation comparison*, SignViP outperforms all competing methods, including SignGAN [61], its enhanced version using AnimateAnyone [29], and SignGen [47]. These results validate SignViP as a more reliable solution for SLVG by effectively preserving semantic consistency. As shown in Table 2, in *pose back-translation comparison*, SignViP consistently outperforms previous SLVG methods and SLP methods (*i.e.*, ProTran [58], Adversarial Training [56], and MDN [60]) across most evaluation metrics. Although MoMP [59] achieves slightly higher scores than our SignViP on certain metrics, our method remains highly competitive overall. It is worth noting that these SLP baselines translate text directly into pose sequences, which aligns with our pose back-translation evaluation pipeline. In contrast, our SLVG method requires detecting poses from the generated videos, potentially introducing additional errors that could impact evaluation results. To enable a more fair comparison under the SLVG setting, we further combine the state-of-the-art SLP method, MoMP, with a pose-to-video generation approach (*i.e.*, ControlNet [88] or AnimateAnyone [29]). As shown in the first two rows of Table 1, the video back-translation results demonstrate that our method is better suited for the SLVG task compared to MoMP-based methods. These results further underscore SignViP’s effectiveness in preserving semantic accuracy.

Video Quality Comparison. Table 3 summarizes the video quality comparison of the generated sign language videos. Our proposed SignViP method significantly outperforms prior SLVG approaches across all evaluated metrics. Specifically, the lowest FID, CLIP-FID, and FVD achieved by our model demonstrate its superior ability to generate sign language videos that are not only visually realistic but also exhibit high temporal coherence and natural motion consistency. Furthermore, the highest IDS scores achieved by our method highlight its effectiveness in accurately preserving the identity of the signer. These results collectively validate the efficacy of SignViP in producing high-fidelity, visually coherent, and perceptually realistic sign language videos.

Generative Capability Comparison for Video Diffusion Models. To compare the generative capabilities of different video diffusion models, we evaluate three methods, which are ControlNet [88], AnimateAnyone [29], and our Sign Video Diffusion Model. As detailed in Table 4, our Sign Video Diffusion Model consistently outperforms other methods across all metrics. Specifically, our Hand SSIM outperforms others, highlighting our model’s ability to preserve hand details. The results clearly highlight the superiority of our method.

Qualitative Comparison. We present the qualitative results in Figure 3(a) of the previous SLVG methods and our SignViP. Compared to the previous methods, SignViP generates higher-quality sign language videos while maintaining greater semantic accuracy with the spoken language text.

Table 3: Comparison of video quality.

| | RWTH-2014T | | | | How2Sign | | | |
|-----------------------|---------------|---------------|----------------|--------------|---------------|---------------|----------------|--------------|
| | FID ↓ | CLIP-FID ↓ | FVD ↓ | IDS ↑ | FID ↓ | CLIP-FID ↓ | FVD ↓ | IDS ↑ |
| SignGAN [61] | 547.90 | 167.70 | 1431.38 | 0.463 | 667.44 | 210.11 | 2766.97 | 0.538 |
| w/ AnimateAnyone [29] | 595.99 | 161.97 | 1330.54 | 0.462 | 679.41 | 215.05 | 2484.39 | 0.533 |
| SignGen [47] | 644.06 | 184.66 | 1715.32 | 0.515 | 815.69 | 186.32 | 3538.49 | 0.539 |
| SignViP (Ours) | 508.91 | 154.10 | 1025.45 | 0.571 | 575.67 | 109.61 | 2207.67 | 0.624 |

Table 4: Generative capability comparison of video diffusion models.

| | RWTH-2014T | | | | | How2Sign | | | | |
|--|---------------|--------------|--------------|--------------|--------------|---------------|--------------|--------------|--------------|--------------|
| | FVD ↓ | SSIM ↑ | PSNR ↑ | LPIPS ↓ | Hand SSIM ↑ | FVD ↓ | SSIM ↑ | PSNR ↑ | LPIPS ↓ | Hand SSIM ↑ |
| ControlNet [88] | 556.63 | 0.784 | 19.50 | 0.137 | 0.483 | 427.22 | 0.826 | 21.32 | 0.116 | 0.657 |
| AnimateAnyone [29] | 365.42 | 0.794 | 20.06 | 0.121 | 0.505 | 293.18 | 0.821 | 21.54 | 0.103 | 0.663 |
| Sign Video Diffusion Model (Ours) | 275.22 | 0.829 | 22.91 | 0.089 | 0.614 | 210.63 | 0.855 | 23.11 | 0.074 | 0.752 |

4.3 Model Study

Identity Generalization. Figure 3(b) showcases how our SignViP generalizes signer identities by adapting appearance guidance from distinct reference images. This demonstrates the robustness of our method in preserving signer-specific appearances while ensuring accurate sign language translation.

Effect of Multiple Conditions. To evaluate whether incorporating multiple fine-grained conditions improves video quality, we ablate the fine-grained poses and 3D hands from our pipeline, respectively. As shown in Table 5, removing one of the conditions leads to a substantial performance degradation across all metrics. These results demonstrate that incorporating multiple fine-grained conditions is essential for enhancing both the semantic accuracy and visual quality of the generated videos.

Table 5: Effect of multiple conditions.

| | FVD | Hand SSIM | BLEU-4 | ROUGE-L |
|----------------------------|---------------|--------------|-------------|--------------|
| w/o 3D Hands | 382.64 | 0.477 | 5.39 | 23.98 |
| w/o Fine-Grained Poses | 461.98 | 0.488 | 3.13 | 19.41 |
| Multiple Conditions | 275.22 | 0.614 | 8.65 | 28.85 |

Effect of Compression. To investigate the necessity of compression for SignViP, we conduct experiments to assess the impact of the compression/downsampling rate in the FSQ Autoencoder. As illustrated in Figure 4(a), the performance of back-translation improves notably as the compression rate increases. Notably, when the compression rate is set to 1 (*i.e.*, no compression is applied), the model demonstrates significantly poor performance. These results underscore the critical role of compression in enhancing the effectiveness of SignViP.

Effect of Quantization. To investigate the necessity of quantization for SignViP, we conduct an experiment where FSQ is not performed during FSQ Autoencoder, while Multi-Condition Token Translator is trained with continuous embedding prediction. As illustrated in Figure 3(c), we observed that continuous embedding prediction poses significant challenges for the translator, resulting in weak semantic alignment and low video quality. When incorporating FSQ, we achieve substantial improved performance. These findings highlight the importance of quantization for our SignViP.

Effect of Condition Augmentation. To evaluate the impact of condition augmentation (Section 3.4) on generation quality, we conducted experiments by varying the augmentation probability p . Figure 4(b) presents the results of condition augmentation with varying values of p . Specifically, introducing a small probability of augmentation (*i.e.*, $p = 10^{-3}$) slightly improves FVD and ROUGE-L scores, suggesting enhanced video quality and linguistic consistency. However, as p increases further, the effectiveness of condition augmentation diminishes. These results indicate that excessive augmentation introduces too much randomness, impacting both video quality and textual coherence.

Effect of Scheduled Sampling Strategy. To evaluate the effect of varying the sampling ratio r of the scheduled sampling strategy (Section 3.6) on generation quality, we conducted experiments by varying r . The experimental results, as shown in Figure 4(c), reveal that the scheduled sampling strategy significantly impacts the quality of generated outputs. When $r = 1$, meaning all input tokens are replaced with random indices, the results indicate that excessive randomness severely hurts the model’s consistency and coherence. As r decreases, generation quality improves steadily. The best performance is observed at $r = 0.4$. However, as r is further reduced to 0.2, performance begins to

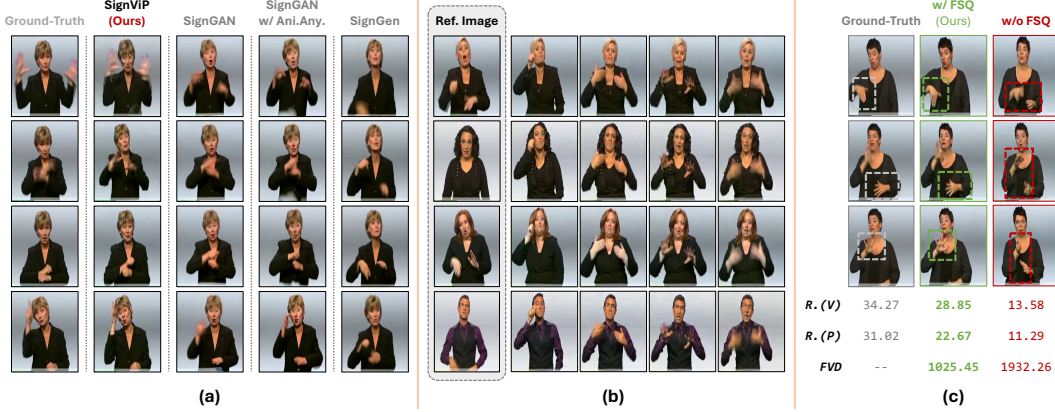


Figure 3: (a) Qualitative comparison on RWTH-2014T dataset. (b) Visual examples illustrating our SignViP’s capability for identity generalization. (c) Effect of quantization. “ $R.(V)$ ” and “ $R.(P)$ ” mean ROUGE metrics of video and pose back-translation, as shown in Table 1 and Table 2, respectively. “FVD” evaluates the protocol described in Table 3.

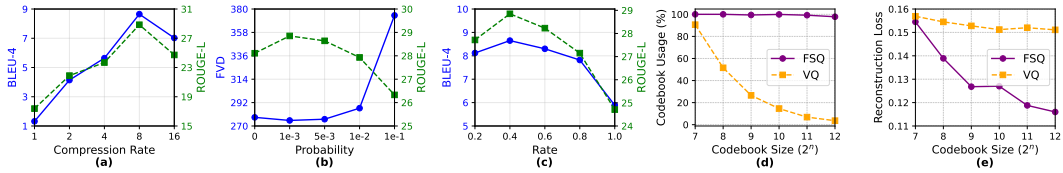


Figure 4: (a) Effect of compression rate. (b) Effect of condition augmentation probability. Note that “FVD” evaluates the protocol described in Table 4. (c) Effect of sampling rate for the scheduled sampling strategy. (d) Codebook usage comparison between FSQ and VQ. (e) Multi-conditional reconstruction loss comparison between FSQ and VQ.

decline slightly. This suggests that a very low replacement ratio is insufficient to simulate the diverse distributions encountered during inference, leading to suboptimal performance.

FSQ vs. VQ. To compare the performance of FSQ with traditional Vector Quantization (VQ), we evaluate both methods in terms of codebook usage efficiency and multi-conditional reconstruction loss. *(1) Codebook Usage.* To assess the efficiency of codebook utilization, we conducted experiments with varying codebook sizes ranging from 2^7 to 2^{12} , and the results are summarized in Figure 4(d). The results demonstrate that FSQ consistently achieves high codebook usage rates, remaining above 97% even with larger codebook. In contrast, VQ experiences a sharp decrease in usage as the codebook size increases. These findings highlight the stability and scalability of FSQ. *(2) Reconstruction Loss.* To evaluate the ability of conditional preservation, we measured the reconstruction loss of both methods under different codebook sizes, as detailed in Figure 4(e). The results show that FSQ achieves consistently lower reconstruction loss compared to VQ, demonstrating its superior capability in preserving original conditional structure.

5 Conclusion

In this work, we propose SignViP, a novel Sign Language Video Generation (SLVG) framework that incorporates multiple fine-grained conditions to enhance generation fidelity by adopting a discrete tokenization paradigm. SignViP consists of three components: (1) Sign Video Diffusion Model, which learns continuous embeddings encapsulating fine-grained motion and appearance details, (2) FSQ Autoencoder, which compresses and quantizes these embeddings into discrete tokens for compact representation, and (3) Multi-Condition Token Translator, which translates spoken language text to discrete multi-condition tokens. Experimental results demonstrate that SignViP achieves state-of-the-art performance in video quality, temporal coherence, and semantic fidelity.

Acknowledgments

We would like to thank the anonymous reviewers for their insightful comments. This work is supported by the JiangSu Natural Science Foundation under Grant No. BK20251989; the National Natural Science Foundation of China under Grants Nos. 62172208, 62441225, 61972192; the Fundamental Research Funds for the Central Universities under Grant No. 14380001. This work is partially supported by Collaborative Innovation Center of Novel Software Technology and Industrialization.

References

- [1] Duarte M Alves, José Pombal, Nuno M Guerreiro, Pedro H Martins, João Alves, Amin Farajian, Ben Peters, Ricardo Rei, Patrick Fernandes, Sweta Agrawal, et al. Tower: An open multilingual large language model for translation-related tasks. *arXiv preprint arXiv:2402.17733*, 2024.
- [2] Guha Balakrishnan, Amy Zhao, Adrian V Dalca, Fredo Durand, and John Guttag. Synthesizing images of humans in unseen poses. In *CVPR*, 2018.
- [3] Vasileios Baltatzis, Rolando Alexandros Potamias, Evangelos Ververas, Guanxiong Sun, Jiankang Deng, and Stefanos Zafeiriou. Neural sign actors: a diffusion model for 3d sign language production from text. In *CVPR*, 2024.
- [4] Andreas Blattmann, Tim Dockhorn, Sumith Kulal, Daniel Mendelevitch, Maciej Kilian, Dominik Lorenz, Yam Levi, Zion English, Vikram Voleti, Adam Letts, et al. Stable video diffusion: Scaling latent video diffusion models to large datasets. *arXiv preprint arXiv:2311.15127*, 2023.
- [5] Necati Cihan Camgoz, Simon Hadfield, Oscar Koller, Hermann Ney, and Richard Bowden. Neural sign language translation. In *CVPR*, 2018.
- [6] Necati Cihan Camgoz, Oscar Koller, Simon Hadfield, and Richard Bowden. Sign language transformers: Joint end-to-end sign language recognition and translation. In *CVPR*, 2020.
- [7] Zhe Cao, Tomas Simon, Shih-En Wei, and Yaser Sheikh. Realtime multi-person 2d pose estimation using part affinity fields. In *Proceedings of the IEEE conference on computer vision and pattern recognition*, pages 7291–7299, 2017.
- [8] Zifeng Cheng, Zhonghui Wang, Yuchen Fu, Zhiwei Jiang, Yafeng Yin, Cong Wang, and Qing Gu. Contrastive prompting enhances sentence embeddings in llms through inference-time steering. *arXiv preprint arXiv:2505.12831*, 2025.
- [9] Enric Corona, Andrei Zanfir, Eduard Gabriel Bazavan, Nikos Kolotouros, Thiemo Alldieck, and Cristian Sminchisescu. Vlogger: Multimodal diffusion for embodied avatar synthesis. *arXiv preprint arXiv:2403.08764*, 2024.
- [10] Yu Deng, Jiaolong Yang, Dong Chen, Fang Wen, and Xin Tong. Disentangled and controllable face image generation via 3d imitative-contrastive learning. In *CVPR*, 2020.
- [11] Amanda Duarte, Shruti Palaskar, Lucas Ventura, Deepti Ghadiyaram, Kenneth DeHaan, Florian Metze, Jordi Torres, and Xavier Giro-i Nieto. How2sign: a large-scale multimodal dataset for continuous american sign language. In *CVPR*, 2021.
- [12] Stefan Elfwing, Eiji Uchibe, and Kenji Doya. Sigmoid-weighted linear units for neural network function approximation in reinforcement learning. *Neural networks*, 107:3–11, 2018.
- [13] Fernando A Fardo, Victor H Conforto, Francisco C de Oliveira, and Paulo S Rodrigues. A formal evaluation of psnr as quality measurement parameter for image segmentation algorithms. *arXiv preprint arXiv:1605.07116*, 2016.
- [14] Shiwei Gan, Yafeng Yin, Zhiwei Jiang, Lei Xie, and Sanglu Lu. Skeleton-aware neural sign language translation. In *ACM MM*, 2021.
- [15] Shiping Ge, Qiang Chen, Zhiwei Jiang, Yafeng Yin, Liu Qin, Ziyao Chen, and Qing Gu. Implicit location-caption alignment via complementary masking for weakly-supervised dense video captioning. In *AAAI*, 2025.
- [16] Shiping Ge, Zhiwei Jiang, Yafeng Yin, Cong Wang, Zifeng Cheng, and Qing Gu. Fine-grained alignment network for zero-shot cross-modal retrieval. *ACM Transactions on Multimedia Computing, Communications and Applications*, 2025.

[17] Ian Goodfellow, Jean Pouget-Abadie, Mehdi Mirza, Bing Xu, David Warde-Farley, Sherjil Ozair, Aaron Courville, and Yoshua Bengio. Generative adversarial nets. *NeurIPS*, 2014.

[18] Robert Gray. Vector quantization. *IEEE Assp Magazine*, 1984.

[19] Nuno M Guerreiro, Duarte M Alves, Jonas Waldendorf, Barry Haddow, Alexandra Birch, Pierre Colombo, and André FT Martins. Hallucinations in large multilingual translation models. *Transactions of the Association for Computational Linguistics*, 11:1500–1517, 2023.

[20] Dan Guo, Wengang Zhou, Houqiang Li, and Meng Wang. Hierarchical lstm for sign language translation. In *AAAI*, 2018.

[21] Yuwei Guo, Ceyuan Yang, Anyi Rao, Zhengyang Liang, Yaohui Wang, Yu Qiao, Maneesh Agrawala, Duhua Lin, and Bo Dai. Animatediff: Animate your personalized text-to-image diffusion models without specific tuning. *arXiv preprint arXiv:2307.04725*, 2023.

[22] Kaiming He, Xiangyu Zhang, Shaoqing Ren, and Jian Sun. Deep residual learning for image recognition. In *CVPR*, 2016.

[23] Yingqing He, Tianyu Yang, Yong Zhang, Ying Shan, and Qifeng Chen. Latent video diffusion models for high-fidelity long video generation. *arXiv preprint arXiv:2211.13221*, 2022.

[24] Zhiwei He, Tian Liang, Wenxiang Jiao, Zhuosheng Zhang, Yujiu Yang, Rui Wang, Zhaopeng Tu, Shuming Shi, and Xing Wang. Exploring human-like translation strategy with large language models. *Transactions of the Association for Computational Linguistics*, 12:229–246, 2024.

[25] Dan Hendrycks and Kevin Gimpel. Gaussian error linear units (gelus). *arXiv preprint arXiv:1606.08415*, 2016.

[26] Martin Heusel, Hubert Ramsauer, Thomas Unterthiner, Bernhard Nessler, and Sepp Hochreiter. Gans trained by a two time-scale update rule converge to a local nash equilibrium. *Advances in neural information processing systems*, 30, 2017.

[27] Jonathan Ho and Tim Salimans. Classifier-free diffusion guidance. *arXiv preprint arXiv:2207.12598*, 2022.

[28] Jonathan Ho, Ajay Jain, and Pieter Abbeel. Denoising diffusion probabilistic models. In *NeurIPS*, 2020.

[29] Li Hu. Animate anyone: Consistent and controllable image-to-video synthesis for character animation. In *CVPR*, 2024.

[30] Diederik P Kingma. Adam: A method for stochastic optimization. *arXiv preprint arXiv:1412.6980*, 2014.

[31] Diederik P Kingma and Max Welling. Auto-encoding variational bayes. *arXiv preprint arXiv:1312.6114*, 2013.

[32] Oscar Koller, Sepehr Zargaran, and Hermann Ney. Re-sign: Re-aligned end-to-end sequence modelling with deep recurrent cnn-hmm. In *CVPR*, 2017.

[33] Marek Kowalski, Stephan J Garbin, Virginia Estellers, Tadas Baltrušaitis, Matthew Johnson, and Jamie Shotton. Config: Controllable neural face image generation. In *ECCV*, 2020.

[34] Chin-Yew Lin and Franz Josef Och. Automatic evaluation of machine translation quality using longest common subsequence and skip-bigram statistics. In *ACL*, 2004.

[35] Yahui Liu, Marco De Nadai, Gloria Zen, Nicu Sebe, and Bruno Lepri. Gesture-to-gesture translation in the wild via category-independent conditional maps. In *ACM MM*, 2019.

[36] Cheng Lu, Yuhao Zhou, Fan Bao, Jianfei Chen, Chongxuan Li, and Jun Zhu. Dpm-solver: A fast ode solver for diffusion probabilistic model sampling in around 10 steps. *NeurIPS*, 2022.

[37] Cheng Lu, Yuhao Zhou, Fan Bao, Jianfei Chen, Chongxuan Li, and Jun Zhu. Dpm-solver++: Fast solver for guided sampling of diffusion probabilistic models. *arXiv preprint arXiv:2211.01095*, 2022.

[38] Liqian Ma, Xu Jia, Qianru Sun, Bernt Schiele, Tinne Tuytelaars, and Luc Van Gool. Pose guided person image generation. *NeurIPS*, 2017.

[39] Yue Ma, Yingqing He, Xiaodong Cun, Xintao Wang, Siran Chen, Xiu Li, and Qifeng Chen. Follow your pose: Pose-guided text-to-video generation using pose-free videos. In *AAAI*, 2024.

[40] Yifang Men, Yiming Mao, Yuning Jiang, Wei-Ying Ma, and Zhouhui Lian. Controllable person image synthesis with attribute-decomposed gan. In *CVPR*, 2020.

[41] Fabian Mentzer, David Minnen, Eirikur Agustsson, and Michael Tschannen. Finite scalar quantization: Vq-vae made simple. *arXiv preprint arXiv:2309.15505*, 2023.

[42] Alptekin Orbay and Lale Akarun. Neural sign language translation by learning tokenization. In *FG*, 2020.

[43] Foivos Paraperas Papantoniou, Alexandros Lattas, Stylianos Moschoglou, Jiankang Deng, Bernhard Kainz, and Stefanos Zafeiriou. Arc2face: A foundation model for id-consistent human faces. In *ECCV*, 2024.

[44] Kishore Papineni, Salim Roukos, Todd Ward, and Wei-Jing Zhu. Bleu: a method for automatic evaluation of machine translation. In *ACL*, 2002.

[45] Junfu Pu, Wengang Zhou, and Houqiang Li. Iterative alignment network for continuous sign language recognition. In *CVPR*, 2019.

[46] Delong Qi, Weijun Tan, Qi Yao, and Jingfeng Liu. Yolo5face: Why reinventing a face detector. In *ECCV*, 2022.

[47] Fan Qi, Yu Duan, Huaiwen Zhang, and Changsheng Xu. Signgen: End-to-end sign language video generation with latent diffusion. In *ECCV*, 2024.

[48] Alec Radford, Jeffrey Wu, Rewon Child, David Luan, Dario Amodei, Ilya Sutskever, et al. Language models are unsupervised multitask learners. *OpenAI blog*, 1(8):9, 2019.

[49] Alec Radford, Jong Wook Kim, Chris Hallacy, Aditya Ramesh, Gabriel Goh, Sandhini Agarwal, Girish Sastry, Amanda Askell, Pamela Mishkin, Jack Clark, et al. Learning transferable visual models from natural language supervision. In *ICML*, 2021.

[50] Prajit Ramachandran, Barret Zoph, and Quoc V Le. Swish: a self-gated activation function. *arXiv preprint arXiv:1710.05941*, 7(1):5, 2017.

[51] Ricardo Rei, Craig Stewart, Ana C Farinha, and Alon Lavie. Comet: A neural framework for mt evaluation. *arXiv preprint arXiv:2009.09025*, 2020.

[52] Ricardo Rei, José GC De Souza, Duarte Alves, Chrysoula Zerva, Ana C Farinha, Taisiya Glushkova, Alon Lavie, Luisa Coheur, and André FT Martins. Comet-22: Unbabel-ist 2022 submission for the metrics shared task. In *Proceedings of the Seventh Conference on Machine Translation (WMT)*, pages 578–585, 2022.

[53] Yixuan Ren, Yang Zhou, Jimei Yang, Jing Shi, Difan Liu, Feng Liu, Mingi Kwon, and Abhinav Shrivastava. Customize-a-video: One-shot motion customization of text-to-video diffusion models. In *ECCV*, 2024.

[54] Danilo Jimenez Rezende, Shakir Mohamed, and Daan Wierstra. Stochastic backpropagation and approximate inference in deep generative models. In *ICML*, 2014.

[55] Robin Rombach, Andreas Blattmann, Dominik Lorenz, Patrick Esser, and Björn Ommer. High-resolution image synthesis with latent diffusion models. In *CVPR*, 2022.

[56] Ben Saunders, Necati Cihan Camgoz, and Richard Bowden. Adversarial training for multi-channel sign language production. *arXiv preprint arXiv:2008.12405*, 2020.

[57] Ben Saunders, Necati Cihan Camgoz, and Richard Bowden. Everybody sign now: Translating spoken language to photo realistic sign language video. *arXiv preprint arXiv:2011.09846*, 2020.

[58] Ben Saunders, Necati Cihan Camgoz, and Richard Bowden. Progressive transformers for end-to-end sign language production. In *ECCV*, 2020.

[59] Ben Saunders, Necati Cihan Camgoz, and Richard Bowden. Mixed signals: Sign language production via a mixture of motion primitives. In *CVPR*, 2021.

[60] Ben Saunders, Necati Cihan Camgoz, and Richard Bowden. Continuous 3d multi-channel sign language production via progressive transformers and mixture density networks. *IJCV*, 2021.

[61] Ben Saunders, Necati Cihan Camgoz, and Richard Bowden. Signing at scale: Learning to co-articulate signs for large-scale photo-realistic sign language production. In *CVPR*, 2022.

[62] Fei Shen and Jinhui Tang. Imagpose: A unified conditional framework for pose-guided person generation. *NeurIPS*, 2024.

[63] Fei Shen, Hu Ye, Jun Zhang, Cong Wang, Xiao Han, and Wei Yang. Advancing pose-guided image synthesis with progressive conditional diffusion models. *arXiv preprint arXiv:2310.06313*, 2023.

[64] Fei Shen, Xiaoyu Du, Yutong Gao, Jian Yu, Yushe Cao, Xing Lei, and Jinhui Tang. Imagharmony: Controllable image editing with consistent object quantity and layout. *arXiv preprint arXiv:2506.01949*, 2025.

[65] Fei Shen, Xin Jiang, Xin He, Hu Ye, Cong Wang, Xiaoyu Du, Zechao Li, and Jinhui Tang. Imagdressing-v1: Customizable virtual dressing. In *AAAI*, 2025.

[66] Fei Shen, Cong Wang, Junyao Gao, Qin Guo, Jisheng Dang, Jinhui Tang, and Tat-Seng Chua. Long-term talkingface generation via motion-prior conditional diffusion model. *arXiv preprint arXiv:2502.09533*, 2025.

[67] Fei Shen, Hu Ye, Sibo Liu, Jun Zhang, Cong Wang, Xiao Han, and Yang Wei. Boosting consistency in story visualization with rich-contextual conditional diffusion models. In *AAAI*, 2025.

[68] Fei Shen, Jian Yu, Cong Wang, Xin Jiang, Xiaoyu Du, and Jinhui Tang. Imaggarment-1: Fine-grained garment generation for controllable fashion design. *arXiv preprint arXiv:2504.13176*, 2025.

[69] Tongkai Shi, Lianyu Hu, Fanhua Shang, Jichao Feng, Peidong Liu, and Wei Feng. Pose-guided fine-grained sign language video generation. In *ECCV*, 2024.

[70] Jascha Sohl-Dickstein, Eric Weiss, Niru Maheswaranathan, and Surya Ganguli. Deep unsupervised learning using nonequilibrium thermodynamics. In *ICML*, 2015.

[71] Jiaming Song, Chenlin Meng, and Stefano Ermon. Denoising diffusion implicit models. *arXiv preprint arXiv:2010.02502*, 2020.

[72] Yang Song, Prafulla Dhariwal, Mark Chen, and Ilya Sutskever. Consistency models. In *ICML*, 2023.

[73] Hao Tang, Wei Wang, Dan Xu, Yan Yan, and Nicu Sebe. Gesturegan for hand gesture-to-gesture translation in the wild. In *ACM MM*, 2018.

[74] Thomas Unterthiner, Sjoerd Van Steenkiste, Karol Kurach, Raphael Marinier, Marcin Michalski, and Sylvain Gelly. Towards accurate generative models of video: A new metric & challenges. *arXiv preprint arXiv:1812.01717*, 2018.

[75] Aaron Van Den Oord, Oriol Vinyals, et al. Neural discrete representation learning. *NeurIPS*, 2017.

[76] Ashish Vaswani, Noam Shazeer, Niki Parmar, Jakob Uszkoreit, Llion Jones, Aidan N Gomez, Łukasz Kaiser, and Illia Polosukhin. Attention is all you need. *NeurIPS*, 2017.

[77] Cong Wang, Kuan Tian, Jun Zhang, Yonghang Guan, Feng Luo, Fei Shen, Zhiwei Jiang, Qing Gu, Xiao Han, and Wei Yang. V-express: Conditional dropout for progressive training of portrait video generation. *arXiv preprint arXiv:2406.02511*, 2024.

[78] Cong Wang, Kuan Tian, Yonghang Guan, Fei Shen, Zhiwei Jiang, Qing Gu, and Jun Zhang. Ensembling diffusion models via adaptive feature aggregation. In *ICLR*, 2025.

[79] Ting-Chun Wang, Ming-Yu Liu, Jun-Yan Zhu, Guilin Liu, Andrew Tao, Jan Kautz, and Bryan Catanzaro. Video-to-video synthesis. *arXiv preprint arXiv:1808.06601*, 2018.

[80] Ting-Chun Wang, Ming-Yu Liu, Jun-Yan Zhu, Andrew Tao, Jan Kautz, and Bryan Catanzaro. High-resolution image synthesis and semantic manipulation with conditional gans. In *CVPR*, 2018.

[81] Zhou Wang, Alan C Bovik, Hamid R Sheikh, and Eero P Simoncelli. Image quality assessment: from error visibility to structural similarity. *IEEE TIP*, 2004.

[82] Mengting Wei, Yante Li, Tuomas Varanka, Yan Jiang, Licai Sun, and Guoying Zhao. Magicportrait: Temporally consistent face reenactment with 3d geometric guidance. *arXiv preprint arXiv:2504.21497*, 2025.

[83] Pan Xie, Qipeng Zhang, Peng Taiying, Hao Tang, Yao Du, and Zexian Li. G2p-ddm: Generating sign pose sequence from gloss sequence with discrete diffusion model. In *AAAI*, 2024.

[84] Zhongcong Xu, Jianfeng Zhang, Jun Hao Liew, Hanshu Yan, Jia-Wei Liu, Chenxu Zhang, Jiashi Feng, and Mike Zheng Shou. Magicanimate: Temporally consistent human image animation using diffusion model. In *CVPR*, 2024.

- [85] Jingyun Xue, Hongfa Wang, Qi Tian, Yue Ma, Andong Wang, Zhiyuan Zhao, Shaobo Min, Wenzhe Zhao, Kaihao Zhang, Heung-Yeung Shum, et al. Follow-your-pose v2: Multiple-condition guided character image animation for stable pose control. *arXiv preprint arXiv:2406.03035*, 2024.
- [86] Aoxiong Yin, Haoyuan Li, Kai Shen, Siliang Tang, and Yueling Zhuang. T2s-gpt: Dynamic vector quantization for autoregressive sign language production from text. *arXiv preprint arXiv:2406.07119*, 2024.
- [87] Jan Zelinka and Jakub Kanis. Neural sign language synthesis: Words are our glosses. In *WACV*, 2020.
- [88] Lvmin Zhang, Anyi Rao, and Maneesh Agrawala. Adding conditional control to text-to-image diffusion models. In *CVPR*, 2023.
- [89] Richard Zhang, Phillip Isola, Alexei A Efros, Eli Shechtman, and Oliver Wang. The unreasonable effectiveness of deep features as a perceptual metric. In *CVPR*, 2018.
- [90] Hao Zhou, Wengang Zhou, Yun Zhou, and Houqiang Li. Spatial-temporal multi-cue network for continuous sign language recognition. In *AAAI*, 2020.
- [91] Jingkai Zhou, Benzhi Wang, Weihua Chen, Jingqi Bai, Dongyang Li, Aixi Zhang, Hao Xu, Mingyang Yang, and Fan Wang. Realisdance: Equip controllable character animation with realistic hands. *arXiv preprint arXiv:2409.06202*, 2024.

NeurIPS Paper Checklist

1. Claims

Question: Do the main claims made in the abstract and introduction accurately reflect the paper's contributions and scope?

Answer: [\[Yes\]](#)

Justification: The main claims made in the abstract and introduction accurately reflect our contributions.

Guidelines:

- The answer NA means that the abstract and introduction do not include the claims made in the paper.
- The abstract and/or introduction should clearly state the claims made, including the contributions made in the paper and important assumptions and limitations. A No or NA answer to this question will not be perceived well by the reviewers.
- The claims made should match theoretical and experimental results, and reflect how much the results can be expected to generalize to other settings.
- It is fine to include aspirational goals as motivation as long as it is clear that these goals are not attained by the paper.

2. Limitations

Question: Does the paper discuss the limitations of the work performed by the authors?

Answer: [\[Yes\]](#)

Justification: We discuss the limitations in supplemental material.

Guidelines:

- The answer NA means that the paper has no limitation while the answer No means that the paper has limitations, but those are not discussed in the paper.
- The authors are encouraged to create a separate "Limitations" section in their paper.
- The paper should point out any strong assumptions and how robust the results are to violations of these assumptions (e.g., independence assumptions, noiseless settings, model well-specification, asymptotic approximations only holding locally). The authors should reflect on how these assumptions might be violated in practice and what the implications would be.
- The authors should reflect on the scope of the claims made, e.g., if the approach was only tested on a few datasets or with a few runs. In general, empirical results often depend on implicit assumptions, which should be articulated.
- The authors should reflect on the factors that influence the performance of the approach. For example, a facial recognition algorithm may perform poorly when image resolution is low or images are taken in low lighting. Or a speech-to-text system might not be used reliably to provide closed captions for online lectures because it fails to handle technical jargon.
- The authors should discuss the computational efficiency of the proposed algorithms and how they scale with dataset size.
- If applicable, the authors should discuss possible limitations of their approach to address problems of privacy and fairness.
- While the authors might fear that complete honesty about limitations might be used by reviewers as grounds for rejection, a worse outcome might be that reviewers discover limitations that aren't acknowledged in the paper. The authors should use their best judgment and recognize that individual actions in favor of transparency play an important role in developing norms that preserve the integrity of the community. Reviewers will be specifically instructed to not penalize honesty concerning limitations.

3. Theory assumptions and proofs

Question: For each theoretical result, does the paper provide the full set of assumptions and a complete (and correct) proof?

Answer: [\[NA\]](#)

Justification: Our paper focuses on experimental work; therefore, it does not include theoretical results.

Guidelines:

- The answer NA means that the paper does not include theoretical results.
- All the theorems, formulas, and proofs in the paper should be numbered and cross-referenced.
- All assumptions should be clearly stated or referenced in the statement of any theorems.
- The proofs can either appear in the main paper or the supplemental material, but if they appear in the supplemental material, the authors are encouraged to provide a short proof sketch to provide intuition.
- Inversely, any informal proof provided in the core of the paper should be complemented by formal proofs provided in appendix or supplemental material.
- Theorems and Lemmas that the proof relies upon should be properly referenced.

4. Experimental result reproducibility

Question: Does the paper fully disclose all the information needed to reproduce the main experimental results of the paper to the extent that it affects the main claims and/or conclusions of the paper (regardless of whether the code and data are provided or not)?

Answer: **[Yes]**

Justification: All the information of reproducibility can be found in Section "Experiments" and Appendix.

Guidelines:

- The answer NA means that the paper does not include experiments.
- If the paper includes experiments, a No answer to this question will not be perceived well by the reviewers: Making the paper reproducible is important, regardless of whether the code and data are provided or not.
- If the contribution is a dataset and/or model, the authors should describe the steps taken to make their results reproducible or verifiable.
- Depending on the contribution, reproducibility can be accomplished in various ways. For example, if the contribution is a novel architecture, describing the architecture fully might suffice, or if the contribution is a specific model and empirical evaluation, it may be necessary to either make it possible for others to replicate the model with the same dataset, or provide access to the model. In general, releasing code and data is often one good way to accomplish this, but reproducibility can also be provided via detailed instructions for how to replicate the results, access to a hosted model (e.g., in the case of a large language model), releasing of a model checkpoint, or other means that are appropriate to the research performed.
- While NeurIPS does not require releasing code, the conference does require all submissions to provide some reasonable avenue for reproducibility, which may depend on the nature of the contribution. For example
 - (a) If the contribution is primarily a new algorithm, the paper should make it clear how to reproduce that algorithm.
 - (b) If the contribution is primarily a new model architecture, the paper should describe the architecture clearly and fully.
 - (c) If the contribution is a new model (e.g., a large language model), then there should either be a way to access this model for reproducing the results or a way to reproduce the model (e.g., with an open-source dataset or instructions for how to construct the dataset).
 - (d) We recognize that reproducibility may be tricky in some cases, in which case authors are welcome to describe the particular way they provide for reproducibility. In the case of closed-source models, it may be that access to the model is limited in some way (e.g., to registered users), but it should be possible for other researchers to have some path to reproducing or verifying the results.

5. Open access to data and code

Question: Does the paper provide open access to the data and code, with sufficient instructions to faithfully reproduce the main experimental results, as described in supplemental material?

Answer: [\[Yes\]](#)

Justification: The supplementary material includes code and data. We will open-source our work after acceptance.

Guidelines:

- The answer NA means that paper does not include experiments requiring code.
- Please see the NeurIPS code and data submission guidelines (<https://nips.cc/public/guides/CodeSubmissionPolicy>) for more details.
- While we encourage the release of code and data, we understand that this might not be possible, so “No” is an acceptable answer. Papers cannot be rejected simply for not including code, unless this is central to the contribution (e.g., for a new open-source benchmark).
- The instructions should contain the exact command and environment needed to run to reproduce the results. See the NeurIPS code and data submission guidelines (<https://nips.cc/public/guides/CodeSubmissionPolicy>) for more details.
- The authors should provide instructions on data access and preparation, including how to access the raw data, preprocessed data, intermediate data, and generated data, etc.
- The authors should provide scripts to reproduce all experimental results for the new proposed method and baselines. If only a subset of experiments are reproducible, they should state which ones are omitted from the script and why.
- At submission time, to preserve anonymity, the authors should release anonymized versions (if applicable).
- Providing as much information as possible in supplemental material (appended to the paper) is recommended, but including URLs to data and code is permitted.

6. Experimental setting/details

Question: Does the paper specify all the training and test details (e.g., data splits, hyper-parameters, how they were chosen, type of optimizer, etc.) necessary to understand the results?

Answer: [\[Yes\]](#)

Justification: Experimental setting and details can be found in Section "Experiments" and Appendix.

Guidelines:

- The answer NA means that the paper does not include experiments.
- The experimental setting should be presented in the core of the paper to a level of detail that is necessary to appreciate the results and make sense of them.
- The full details can be provided either with the code, in appendix, or as supplemental material.

7. Experiment statistical significance

Question: Does the paper report error bars suitably and correctly defined or other appropriate information about the statistical significance of the experiments?

Answer: [\[Yes\]](#)

Justification: The experiments support the main claims of the paper.

Guidelines:

- The answer NA means that the paper does not include experiments.
- The authors should answer “Yes” if the results are accompanied by error bars, confidence intervals, or statistical significance tests, at least for the experiments that support the main claims of the paper.
- The factors of variability that the error bars are capturing should be clearly stated (for example, train/test split, initialization, random drawing of some parameter, or overall run with given experimental conditions).

- The method for calculating the error bars should be explained (closed form formula, call to a library function, bootstrap, etc.)
- The assumptions made should be given (e.g., Normally distributed errors).
- It should be clear whether the error bar is the standard deviation or the standard error of the mean.
- It is OK to report 1-sigma error bars, but one should state it. The authors should preferably report a 2-sigma error bar than state that they have a 96% CI, if the hypothesis of Normality of errors is not verified.
- For asymmetric distributions, the authors should be careful not to show in tables or figures symmetric error bars that would yield results that are out of range (e.g. negative error rates).
- If error bars are reported in tables or plots, The authors should explain in the text how they were calculated and reference the corresponding figures or tables in the text.

8. Experiments compute resources

Question: For each experiment, does the paper provide sufficient information on the computer resources (type of compute workers, memory, time of execution) needed to reproduce the experiments?

Answer: **[Yes]**

Justification: We claim the compute resources in Appendix.

Guidelines:

- The answer NA means that the paper does not include experiments.
- The paper should indicate the type of compute workers CPU or GPU, internal cluster, or cloud provider, including relevant memory and storage.
- The paper should provide the amount of compute required for each of the individual experimental runs as well as estimate the total compute.
- The paper should disclose whether the full research project required more compute than the experiments reported in the paper (e.g., preliminary or failed experiments that didn't make it into the paper).

9. Code of ethics

Question: Does the research conducted in the paper conform, in every respect, with the NeurIPS Code of Ethics <https://neurips.cc/public/EthicsGuidelines>?

Answer: **[Yes]**

Justification: We conducted in the paper conform with the NeurIPS Code of Ethics.

Guidelines:

- The answer NA means that the authors have not reviewed the NeurIPS Code of Ethics.
- If the authors answer No, they should explain the special circumstances that require a deviation from the Code of Ethics.
- The authors should make sure to preserve anonymity (e.g., if there is a special consideration due to laws or regulations in their jurisdiction).

10. Broader impacts

Question: Does the paper discuss both potential positive societal impacts and negative societal impacts of the work performed?

Answer: **[NA]**

Justification: There is no societal impact of the work performed.

Guidelines:

- The answer NA means that there is no societal impact of the work performed.
- If the authors answer NA or No, they should explain why their work has no societal impact or why the paper does not address societal impact.
- Examples of negative societal impacts include potential malicious or unintended uses (e.g., disinformation, generating fake profiles, surveillance), fairness considerations (e.g., deployment of technologies that could make decisions that unfairly impact specific groups), privacy considerations, and security considerations.

- The conference expects that many papers will be foundational research and not tied to particular applications, let alone deployments. However, if there is a direct path to any negative applications, the authors should point it out. For example, it is legitimate to point out that an improvement in the quality of generative models could be used to generate deepfakes for disinformation. On the other hand, it is not needed to point out that a generic algorithm for optimizing neural networks could enable people to train models that generate Deepfakes faster.
- The authors should consider possible harms that could arise when the technology is being used as intended and functioning correctly, harms that could arise when the technology is being used as intended but gives incorrect results, and harms following from (intentional or unintentional) misuse of the technology.
- If there are negative societal impacts, the authors could also discuss possible mitigation strategies (e.g., gated release of models, providing defenses in addition to attacks, mechanisms for monitoring misuse, mechanisms to monitor how a system learns from feedback over time, improving the efficiency and accessibility of ML).

11. Safeguards

Question: Does the paper describe safeguards that have been put in place for responsible release of data or models that have a high risk for misuse (e.g., pretrained language models, image generators, or scraped datasets)?

Answer: [NA]

Justification: The paper poses no such risks.

Guidelines:

- The answer NA means that the paper poses no such risks.
- Released models that have a high risk for misuse or dual-use should be released with necessary safeguards to allow for controlled use of the model, for example by requiring that users adhere to usage guidelines or restrictions to access the model or implementing safety filters.
- Datasets that have been scraped from the Internet could pose safety risks. The authors should describe how they avoided releasing unsafe images.
- We recognize that providing effective safeguards is challenging, and many papers do not require this, but we encourage authors to take this into account and make a best faith effort.

12. Licenses for existing assets

Question: Are the creators or original owners of assets (e.g., code, data, models), used in the paper, properly credited and are the license and terms of use explicitly mentioned and properly respected?

Answer: [Yes]

Justification: We were allowed to use the dataset and cited them in the paper.

Guidelines:

- The answer NA means that the paper does not use existing assets.
- The authors should cite the original paper that produced the code package or dataset.
- The authors should state which version of the asset is used and, if possible, include a URL.
- The name of the license (e.g., CC-BY 4.0) should be included for each asset.
- For scraped data from a particular source (e.g., website), the copyright and terms of service of that source should be provided.
- If assets are released, the license, copyright information, and terms of use in the package should be provided. For popular datasets, paperswithcode.com/datasets has curated licenses for some datasets. Their licensing guide can help determine the license of a dataset.
- For existing datasets that are re-packaged, both the original license and the license of the derived asset (if it has changed) should be provided.

- If this information is not available online, the authors are encouraged to reach out to the asset's creators.

13. New assets

Question: Are new assets introduced in the paper well documented and is the documentation provided alongside the assets?

Answer: [NA]

Justification: This paper does not release new assets.

Guidelines:

- The answer NA means that the paper does not release new assets.
- Researchers should communicate the details of the dataset/code/model as part of their submissions via structured templates. This includes details about training, license, limitations, etc.
- The paper should discuss whether and how consent was obtained from people whose asset is used.
- At submission time, remember to anonymize your assets (if applicable). You can either create an anonymized URL or include an anonymized zip file.

14. Crowdsourcing and research with human subjects

Question: For crowdsourcing experiments and research with human subjects, does the paper include the full text of instructions given to participants and screenshots, if applicable, as well as details about compensation (if any)?

Answer: [NA]

Justification: The paper does not involve crowdsourcing nor research with human subjects.

Guidelines:

- The answer NA means that the paper does not involve crowdsourcing nor research with human subjects.
- Including this information in the supplemental material is fine, but if the main contribution of the paper involves human subjects, then as much detail as possible should be included in the main paper.
- According to the NeurIPS Code of Ethics, workers involved in data collection, curation, or other labor should be paid at least the minimum wage in the country of the data collector.

15. Institutional review board (IRB) approvals or equivalent for research with human subjects

Question: Does the paper describe potential risks incurred by study participants, whether such risks were disclosed to the subjects, and whether Institutional Review Board (IRB) approvals (or an equivalent approval/review based on the requirements of your country or institution) were obtained?

Answer: [NA]

Justification: The paper does not involve crowdsourcing nor research with human subjects.

Guidelines:

- The answer NA means that the paper does not involve crowdsourcing nor research with human subjects.
- Depending on the country in which research is conducted, IRB approval (or equivalent) may be required for any human subjects research. If you obtained IRB approval, you should clearly state this in the paper.
- We recognize that the procedures for this may vary significantly between institutions and locations, and we expect authors to adhere to the NeurIPS Code of Ethics and the guidelines for their institution.
- For initial submissions, do not include any information that would break anonymity (if applicable), such as the institution conducting the review.

16. Declaration of LLM usage

Question: Does the paper describe the usage of LLMs if it is an important, original, or non-standard component of the core methods in this research? Note that if the LLM is used only for writing, editing, or formatting purposes and does not impact the core methodology, scientific rigorosity, or originality of the research, declaration is not required.

Answer: [NA]

Justification: The core method development in this research does not involve LLMs as any important, original, or non-standard components.

Guidelines:

- The answer NA means that the core method development in this research does not involve LLMs as any important, original, or non-standard components.
- Please refer to our LLM policy (<https://neurips.cc/Conferences/2025/LLM>) for what should or should not be described.

A Limitations

In this paper, we propose a novel SLVG framework, SignViP, which demonstrates significant improvements over previous methods. Nevertheless, our framework still has two notable limitations that warrant further investigation.

The first limitation is its inability to support multiple sign languages simultaneously. As different countries have their own unique sign language systems, adapting SignViP for a specific sign language currently requires training a separate model for each. This dependency on independent model training significantly restricts its practicality in real-world applications. Consequently, the development of a unified SLVG system capable of supporting multiple sign languages will be critical for enhancing its versatility and applicability. Addressing this challenge will serve as a key direction in our future research endeavors.

The second limitation pertains to the computational inefficiency inherent in the iterative denoising process of diffusion models. Existing methods, such as the consistency model [72] and efficient ODE solvers [36, 37], offer promising approaches to accelerate the sampling process of diffusion-based models. Incorporating these techniques into SignViP represents another avenue for improving its efficiency and scalability, which will also be prioritized in our future research.

B Architecture Details

Multi-Condition Encoder. The multi-condition token space in our framework is constructed using a multi-condition encoder. This encoder adopts a simple convolutional architecture with 8 convolutional layers with SiLU activation [12, 50], each achieving a $4\times$ spatial downsampling (*i.e.*, $2\times$ along both the height and width axes).

Mixer in Multi-Condition Token Translator. In Multi-Condition Token Translator, we use a mixer to aggregate tokens from the same frame into unified input hidden states. The mixer consists of a linear layer, followed by LayerNorm and GELU activation [25]. Tokens are first projected into embeddings, which are then flattened and passed through the mixer to produce a single hidden state for each frame.

Decoder in Multi-Condition Token Translator. In the Multi-Condition Token Translator, we utilize a decoder to decode all tokens of the same frame from the output hidden states of the GPT-2 model. The decoder employs multiple parallel heads to decode each token within the frame. Specifically, each head is implemented as a lightweight Transformer layer [76, 8, 15, 16].

C Training Details of Back-Translation Models

To evaluate the semantic consistency of the generated sign language videos, we follow ProTran [58] to train two SLP models [6] to translate sign language videos (*i.e.*, the video back-translation model) and poses (*i.e.*, the pose back-translation model) into texts, respectively.

Video Back-Translation Model. The video back-translation model is trained using a single NVIDIA RTX A6000 GPU. An Adam optimizer [30] is utilized with a learning rate of 1e-3, and the batch size is set to 32. Validation performance is logged every 5 steps, providing checkpoints throughout the training process. The best-performing model checkpoint is observed at step 10,500.

Pose Back-Translation Model. The pose back-translation model is also trained on a single NVIDIA RTX A6000 GPU. The training configuration mirrors that of the video back-translation model, using an Adam optimizer [30] with a learning rate of 1e-3, a batch size of 32, and validation logged every 5 steps. The optimal model checkpoint is reached at step 5,400.

D Human Evaluation

The evaluation protocol based on back-translation models is highly dependent on the quality of the back-translation system, which may introduce certain biases. Although human evaluation could potentially offer a more reliable solution, recruiting qualified sign language experts presents significant challenges.

To address this limitation, we employ a compromise human evaluation strategy that does not require expert knowledge of sign language. Specifically, we present human evaluators with the ground-truth sign language video, along with several anonymized candidate videos generated by different SLVG methods. Evaluators are instructed as follows: *“Please choose the video where the signer’s actions appear most similar to those in the ground-truth video.”*

For this evaluation, we recruited 10 non-expert participants. Each participant evaluated 25 groups of samples for the RWTH-2014T dataset and 50 groups for the How2Sign dataset, resulting in a total of 250 and 500 votes, respectively. We report the proportion of votes received by each SLVG method in Table 6. Notably, our method, SignViP, achieves the highest vote proportion across both datasets, indicating that SignViP generates sign language videos that are more consistent with the ground-truth references as perceived by human evaluators.

Table 6: Human Evaluation Results on RWTH-2014T and How2Sign datasets.

| | RWTH-2014T | | How2Sign | |
|------------------|------------|--------------|------------|--------------|
| | #Votes | Vote% | #Votes | Vote% |
| <i>TOTAL</i> | 250 | 100.0% | 500 | 100% |
| SignGAN | 25 | 10.0% | 31 | 6.2% |
| w/ AnimateAnyone | 23 | 9.2% | 24 | 4.8% |
| SignGen | 27 | 10.8% | 36 | 7.2% |
| SignViP (Ours) | 175 | 70.0% | 409 | 81.8% |

E More Experiments

E.1 Comparison with Direct Condition Prediction

As stated in Section 1, one of the motivations for introducing the multi-condition token space is the inherent difficulty of directly translating fine-grained attributes. In Figure 1(4), we illustrate examples of direct multi-condition predictions, demonstrating significant discrepancies between ground-truth and predicted results. To quantitatively compare the direct condition prediction approach with our proposed method under the pose back-translation paradigm, we present experimental results in Table 7. The results demonstrate that direct condition prediction performs poorly across all metrics. These results clearly demonstrate that direct multi-condition prediction struggles to effectively model the fine-grained attributes and fails to maintain semantic consistency during the translation process.

Table 7: Comparison of pose back-translation performance between direct condition prediction and our proposed SignViP.

| Methods | RWTH-2014T | | | | | How2Sign | | | | |
|----------------------|------------|--------|--------|--------|-------|----------|--------|--------|--------|-------|
| | BLEU-1 | BLEU-2 | BLEU-3 | BLEU-4 | ROUGE | BLEU-1 | BLEU-2 | BLEU-3 | BLEU-4 | ROUGE |
| Ground-Truth | 30.99 | 18.36 | 12.83 | 9.87 | 31.02 | 24.56 | 14.96 | 10.31 | 7.91 | 24.88 |
| Condition Prediction | 9.27 | 2.23 | 0.80 | 0.32 | 11.64 | 5.39 | 1.63 | 2.26 | 1.13 | 8.12 |
| SignViP (Ours) | 21.94 | 10.06 | 6.32 | 4.61 | 22.67 | 17.35 | 8.28 | 5.41 | 4.42 | 18.23 |

E.2 Efficiency Comparison

To compare the efficiency of our method with other approaches, we conducted experiments measuring the number of model parameters and inference time per frame. As shown in Table 8, the results demonstrate that our SignViP achieves comparable model size and inference time to the diffusion-based baselines. This indicates that our method delivers high-quality video generation without incurring significant additional computational cost, making it an efficient and practical solution for sign language video generation.

E.3 Effectiveness of Pretrained Parameter Initialization

The comparison among methods is fair, as all the diffusion-based SLVG approaches (*i.e.*, SignGAN+AnimateAnyone, SignGen, and our SignViP) are initialized with parameters from existing pretrained diffusion models.

Table 8: Efficiency comparison between diffusion-based baselines and our SignViP.

| | # Parameters | Inference Time (s/frame) |
|-------------------------------|--------------|--------------------------|
| SignGAN w/ AnimateAnyone [29] | 2575.85M | 1.3404 |
| SignGen | 2217.38M | 1.2225 |
| SignViP (Ours) | 2777.92M | 1.2398 |

Training a video generation diffusion model from scratch is extremely challenging due to the high computational costs and slow convergence. Therefore, leveraging pretrained diffusion parameters to initialize customized diffusion models has become a fundamental strategy to significantly accelerate training [23, 4, 53, 21, 39].

To further validate the effectiveness of pretrained parameter initialization, we conducted an ablation study, evaluating the quality of generated videos both with and without pretrained initialization under the same number of training steps. The results, presented in Table 9, clearly demonstrate the substantial advantage of initializing with pretrained parameters.

Table 9: Ablation study on the effect of pretrained initialization.

| | FID ↓ | FVD ↓ |
|-------------------------------------|---------------|----------------|
| w/o Pretrained Initialization | 2278.23 | 3277.20 |
| w/ Pretrained Initialization (Ours) | 508.91 | 1025.45 |

E.4 Order-Preserving Evaluation of Back-Translation Models

To further validate the reliability and comparability of our back-translation models, we conduct **order-preserving experiments**. Specifically, we introduce pose sequences with varying levels of errors and evaluate whether the corresponding output metrics display a consistent ranking that reflects the severity of the errors. In other words, a comparable back-translation model should exhibit a steady degradation in output quality as the degree of input error increases.

To simulate realistic pose errors, we independently apply spatial and temporal perturbations as follows: (1) **Spatial Perturbation**: Additive bias is applied to pose keypoints. To mimic real-world errors while avoiding excessive deformation, we first compute the variance of each keypoint’s coordinates from the dataset. The bias added to each keypoint is sampled from a normal distribution $\mathcal{N}(0, \sigma^2)$, where σ reflects the perturbation intensity. (2) **Temporal Perturbation**: We randomly delete, repeat, or duplicate pose frames at a ratio of p , where p controls the perturbation intensity.

The results of the **pose back-translation model** under both spatial and temporal perturbations are summarized in Figure 5(a) and (b). As shown in the figures, all metrics decrease monotonically as the perturbation intensity increases. This demonstrates that our pose back-translation model is sensitive to varying levels of pose errors and can provide reliable evaluation metrics for comparison.

For the **video back-translation model**, we first synthesize videos from the perturbed poses using AnimateAnyone [29], and then evaluate the corresponding metrics. The results of the video back-translation model under both spatial and temporal perturbations are summarized in Figure 5(c) and (d). Consistent with our findings for the pose model, our video back-translation model also provides reliable evaluation metrics for comparison. Note that since we use AnimateAnyone to synthesize new videos, the metrics without perturbation differ from the ground-truth metrics reported in Table 1.

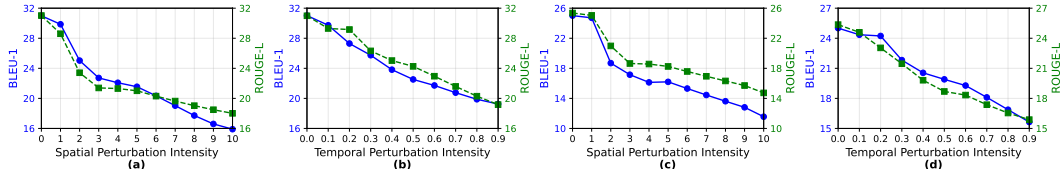


Figure 5: (a) Effect of spatial perturbation for the pose back-translation model. (b) Effect of temporal perturbation for the pose back-translation model. (c) Effect of spatial perturbation for the video back-translation model. (d) Effect of temporal perturbation for the video back-translation model.

F More Cases

We demonstrate more video cases in Figure 6 and Figure 7.



Figure 6: More generated cases of RWTH-2014T dataset.

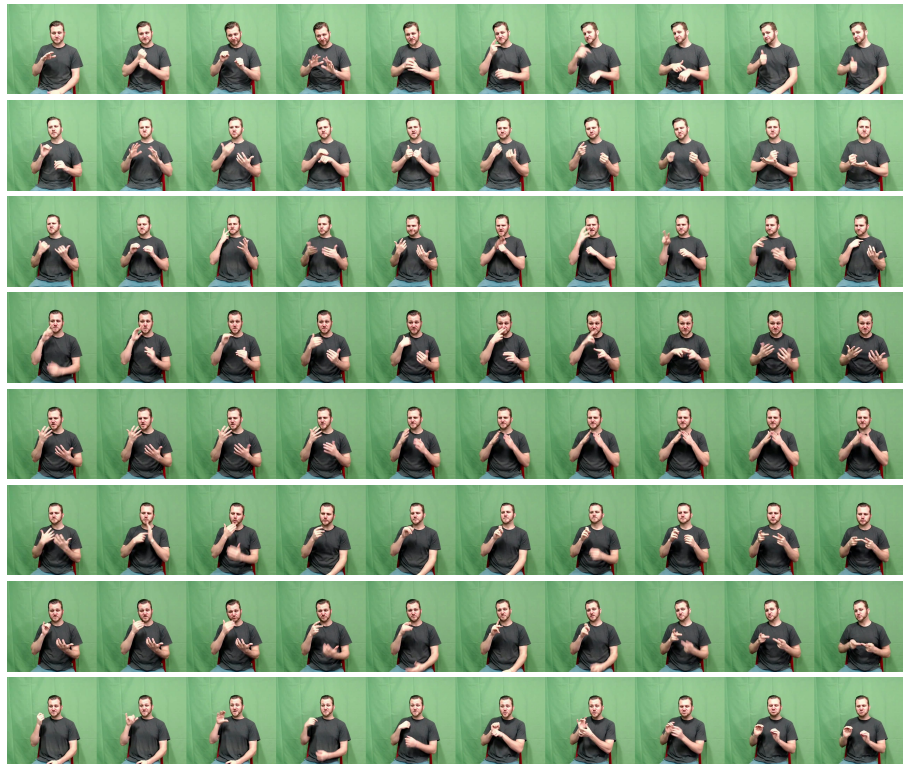


Figure 7: More generated cases of How2Sign dataset.

G Token Translation Accuracy

Directly computing the accuracy of token translation in our framework presents significant challenges. Due to temporal shifts and uneven scaling, translated tokens during inference may not be perfectly aligned with ground-truth tokens, making traditional accuracy metrics less reliable.

To address this, we employ **normalized Dynamic Time Warping (DTW) distance** as an alternative evaluation metric. DTW is a similarity measure that computes the optimal alignment between two sequences, even if they differ in length or are not aligned one-to-one. By normalizing the DTW distance, we accommodate variations in sequence length, enabling fair comparison across different settings. In our evaluation pipeline, we decode the translated tokens into condition embeddings using the decoder of the FSQ Autoencoder, and then compare these embeddings to ground-truth condition embeddings via normalized DTW distance.

To validate the effectiveness of normalized DTW distance as a metric, we conduct experiments following the settings described in “Effect of Compression” and “Effect of Scheduled Sampling Strategy” of Section 4.3. As shown in Tables 10 and 11, the trends of normalized DTW distance closely match those of previously reported metrics (BLEU-4 and ROUGE), confirming its reliability for evaluating token translation accuracy.

Table 10: Effect of Compression Rate on Token Translation Metrics

| Compression Rate | Norm. DTW Distance (↓) | BLEU-4 | ROUGE |
|------------------|------------------------|-------------|--------------|
| 1 | 1.9020 | 1.32 | 17.38 |
| 2 | 1.7937 | 4.14 | 21.89 |
| 4 | 1.7438 | 5.64 | 23.68 |
| 8 (Ours) | 1.5968 | 8.65 | 28.85 |
| 16 | 1.7291 | 7.02 | 24.72 |

Table 11: Effect of Scheduled Sampling Rate on Token Translation Metrics

| Sampling Rate | Norm. DTW Distance (↓) | BLEU-4 | ROUGE |
|-------------------|------------------------|-------------|--------------|
| 0.2 | 1.6123 | 8.12 | 27.72 |
| 0.4 (Ours) | 1.5968 | 8.65 | 28.85 |
| 0.6 | 1.5978 | 8.30 | 28.23 |
| 0.8 | 1.6191 | 7.82 | 27.15 |
| 1.0 | 1.7354 | 5.89 | 24.71 |